Rapid Communications

Reversal of particle-hole scattering-rate asymmetry in the Anderson impurity model

R. Žitko,[1,2] H. R. Krishnamurthy,[3] and B. Sriram Shastry[4]

[1]*Jožef Stefan Institute, Jamova 39, SI-1000 Ljubljana, Slovenia*
[2]*Faculty of Mathematics and Physics, University of Ljubljana, Jadranska 19, SI-1000 Ljubljana, Slovenia*
[3]*Department of Physics, Center for Condensed Matter Theory, Indian Institute of Science, Bengaluru 560012, India*
[4]*Physics Department, University of California, Santa Cruz, California 95064, USA*

We study the particle-hole asymmetry of the scattering rate in strongly correlated electron systems by examining the cubic ω^3 and ωT^2 terms in the imaginary part of the self-energy of the Anderson impurity model. We show that the sign is opposite in the weak-coupling and strong-coupling limits, explaining the differences found in theoretical approaches taking the respective limits as the starting points. The sign change in fact precisely delineates the crossover between the weak- and strong-correlation regimes of the model. For weak interaction U the sign reversal occurs for small values of the doping $\delta = 1 - n$, while for interaction of order $U \approx 2\Gamma$, Γ being the hybridization strength, the crossover curve rapidly shifts to the large-doping range. This curve, based on the impurity dynamics, is genuinely different from other crossover curves defined through impurity thermodynamic and static properties.

In contemporary strongly correlated quantum materials, such as the cuprate superconductors and sodium cobaltates, one finds that spectral line shapes from angle-resolved photoemission spectroscopy (ARPES) differ qualitatively from those in simple Fermi liquids. The origin of the difference has been traced to a large correlation-induced asymmetry in the imaginary part of the self-energy [1,2], which can be expanded as

$$\mathrm{Im}\,\Sigma(\omega, T) = a(\omega^2 + \pi^2 T^2) + b\omega^3 + c\omega T^2 + \cdots. \quad (1)$$

For context, note that the usually quoted Fermi-liquid self-energy, namely, the first two terms in this expression, is *even* in ω. While this is dominant at the lowest energies, the higher-order *odd* in ω terms become important when their coefficients (b, c) become sufficiently large. This is found to happen in the strong-correlation models, while in weakly correlated systems these coefficients are very small. The signs of (b, c) are of particular importance: They determine whether particles or holes have the shorter lifetime. Since $a < 0$, if $b < 0$, the particlelike excitations scatter more strongly on the impurity (are more damped) than the holelike excitations with the same excitation energy (absolute value of ω), and vice versa for $b > 0$. Understanding the asymmetry of the self-energy is a problem of great current interest. The asymmetry of $\mathrm{Im}\,\Sigma$ is relevant to transport coefficients such as the thermopower, where the entropy and charge are carried by both particlelike excitations above the Fermi level and holelike excitations below it. However, in the low-T thermopower there are other competing factors (asymmetry of the density of states, asymmetry of the quasiparticle velocities), hence the situation is not solely controlled by the sign of the scattering asymmetry.

The single-impurity Anderson model (SIAM) is a "laboratory example" of an exactly solvable many-body problem. It is simpler but has many similarities to the lattice many-body problems such as the Hubbard model. It is therefore a natural

place to understand the magnitude and signs of the asymmetric corrections to the lowest-order Fermi-liquid theory result mentioned above. The goal of this Rapid Communication is to explore this asymmetry by using the numerical renormalization group (NRG), and to contrast it with various approximate theories. We report a surprising result in this well-studied problem: We find a line in the U-n plane where the asymmetry changes sign. Here, U is the interaction strength and n the impurity occupancy. Along this one-dimensional line in the U-n plane, the particle-hole (p-h) symmetry of the scattering rate is exactly fulfilled up to the fifth- and higher-order terms. This change of sign demarcates the border between the qualitatively different regimes of weak and strong correlations. Indeed, this Rapid Communication was motivated by the puzzling observation that weak-coupling approaches (e.g., perturbation theory in the interaction strength U) and strong-coupling techniques [e.g., the extremely correlated Fermi-liquid (ECFL) theory [2–4]] give opposite signs for the asymmetry, as illustrated in Fig. 1.

The SIAM is defined by the Hamiltonian

$$H = \epsilon_d(n_\uparrow + n_\downarrow) + Un_\uparrow n_\downarrow$$
$$+ \sum_{k\sigma} \epsilon_k c_{k\sigma}^\dagger c_{k\sigma} + \sum_{k\sigma} (t_k c_{k\sigma}^\dagger d_\sigma + \mathrm{H.c.}), \quad (2)$$

where ϵ_d is the impurity level, d_σ are impurity operators, $n_\sigma = d_\sigma^\dagger d_\sigma$ and $n = \langle n_\uparrow + n_\downarrow \rangle$, and $c_{k\sigma}$ are operators for conduction-band electrons with energy ϵ_k that couple with the impurity with amplitude t_k. The hybridization strength is $\Gamma = \pi \sum_k |t_k|^2 \delta(\omega - \epsilon_k)$; we will assume it to be a constant function in the domain $-D < \omega < D$. In the following we will make use of the Hartree-Fock parameter $E_d = \epsilon_d + U\langle n_\sigma \rangle$ with $E_d = 0$ corresponding to the p-h symmetric $n = 1$ case. We also define the dimensionless interaction $u = U/\pi\Gamma$. We will limit our consideration to $n < 1$, since the results for
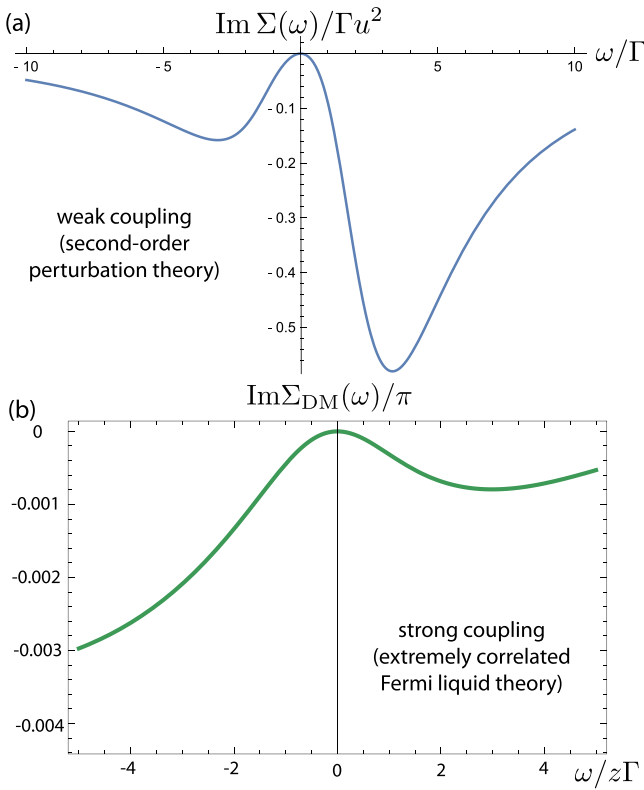
FIG. 1. Imaginary parts of the self-energy in (a) weak-coupling theory and in (b) strong-coupling theory have the opposite sign of the particle-hole asymmetry. The second-order perturbation theory result corresponds to $E_d/\Gamma = 1$ in Fig. 2 of Ref. [5], and the extremely correlated Fermi-liquid theory result to $n = 0.6$ in Fig. 5 of Ref. [4].
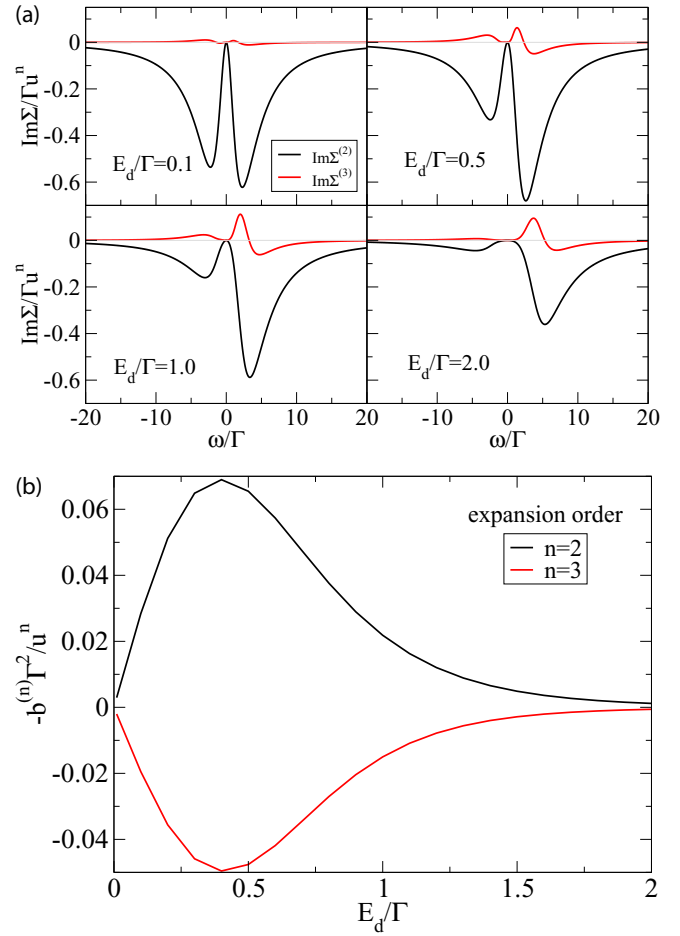

FIG. 2. (a) Second-order and third-order imaginary part of the self-energy for a range of the Hartree-Fock parameters $E_d = \epsilon_d + U\langle n_\sigma \rangle$. The y axis is scaled as $1/(\Gamma u^n)$, where n is the expansion order and $u = U/\pi\Gamma$. $T = 0$. (b) Coefficient b of the ω^3 term in $\mathrm{Im}\,\Sigma(\omega, T = 0)$ at second and third order in perturbation theory.

$n > 1$ can be obtained by the *p-h* transformation $d_\sigma \rightarrow d_\sigma^\dagger$, $c_{k\sigma} \rightarrow -c_{k\sigma}^\dagger$, which takes ω to $-\omega$.

Second-order perturbation theory in U for the SIAM [5] [e.g., Fig. 1(a) for $E_d/\Gamma = 1$] predicts b to be of constant sign as a function of n in the full domain $0 < n < 1$, with zero value at $n = 1$. Specifically, $b < 0$, i.e., the particlelike excitations scatter more strongly. At nonzero but low temperatures, the asymmetry of $\mathrm{Im}\,\Sigma(\omega)$ at low ω will be controlled by the ωT^2 term. Due to conformal symmetry of the FL fixed point, $c = b\pi^2$, thus the sign of the asymmetry does not depend on T at low enough temperatures [6].

By extending the perturbative expansion to third order, we find that the third-order contributions tend to have the opposite sign of the second-order ones for small ω, i.e., they reduce the scattering. Furthermore, the asymmetry of the third-order contribution is such that the $\omega > 0$ part is dominant (for $n < 1$), thus the third-order reduction in scattering is stronger for particlelike excitations [see Fig. 2(a)]. There is thus a competition between the second- and third-order contributions which may lead to a change in sign of the asymmetric terms. The contributions $b^{(2)}$ and $b^{(3)}$ to the coefficient b actually follow very similar qualitative E_d dependence [see Fig. 2(b)], except for the sign and evidently a different power of $u = U/\pi\Gamma$. Based on these results, the change of sign in b should occur for $u \sim 1$, i.e., $U \sim \pi\Gamma$. Since the perturbation theory also breaks down at $u \sim 1$, we cannot make a precise

statement about the details of this sign change within the bare perturbative approach.

We therefore solved the impurity problem numerically using the numerical renormalization group (NRG) [7–12]. This nonperturbative approach is based on logarithmic discretization of the continuum, mapping onto a tight-binding chain with exponentially decreasing hopping constants, and iterative diagonalization of the resulting Hamiltonian [7,8,12]. Through various refinements over the years [11,13–20] the technique has developed into a powerful tool for computing the dynamical properties of impurity models. Comparisons with quantum Monte Carlo simulations indicate that the results of the NRG, when taken to full convergence, may be considered as essentially exact (up to very small systematic errors due to discretization and truncation). We performed the NRG calculations with a narrow broadening kernel by averaging over $N_z = 32$ interleaved discretization grids with the discretization parameter $\Lambda = 2$, and increasing the truncation cutoff until convergence [20]: These steps reduced the oscillatory artifacts and allowed a reliable extraction of the cubic term in the self-energy function in the limit of small
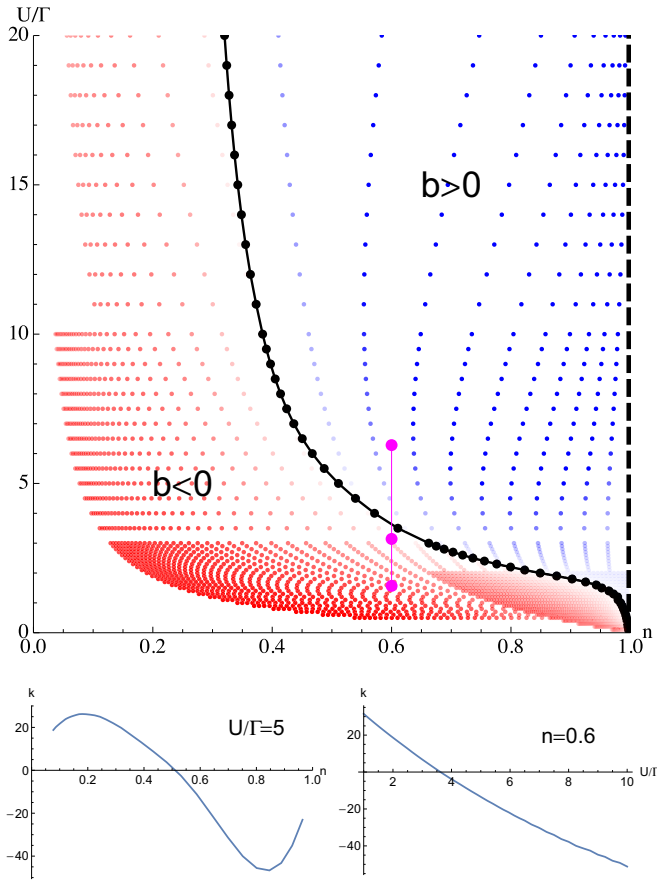
FIG. 3. Top: Sign (red negative, blue positive) and magnitude (color saturation) of the ω^3 term in $\mathrm{Im}\,\Sigma(\omega, T=0)$. The quantity shown is the coefficient k in the fit of the antisymmetrized and normalized combination $[\mathrm{Im}\,\Sigma(\omega) - \mathrm{Im}\,\Sigma(-\omega)]/[\mathrm{Im}\,\Sigma(\omega) + \mathrm{Im}\,\Sigma(-\omega)]$ with the linear function $k\omega$. The fit is performed in an energy interval $\omega \in [-\xi : \xi]$; here, ξ is the low-energy scale of the problem defined as the temperature where the impurity moment is screened (and is equivalent to the Kondo temperature in the Kondo regime of the model). Notice that $k \approx b/a$ and that $a < 0$. The three magenta points joined by a line are considered in Fig. 4. The dashed lined at $n = 1$ indicates a further zero crossing of the coefficient k at the particle-hole symmetric point of the Hamiltonian itself. Bottom: Cross sections at constant interaction $U/\Gamma = 5$ and constant occupancy $n = 0.6$.
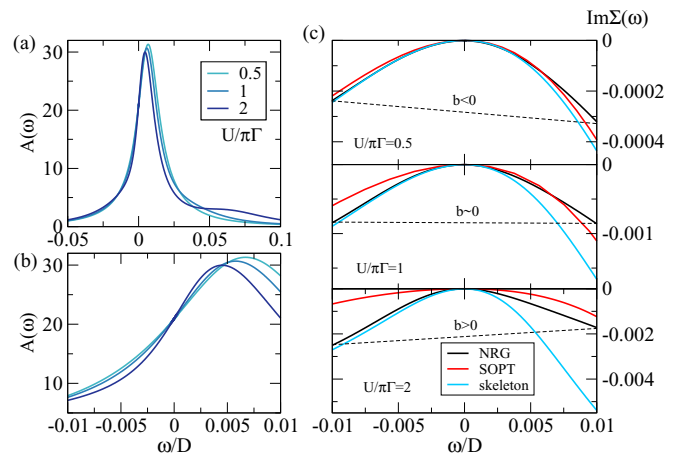

FIG. 4. Spectral function and imaginary part of self-energy for $n = 0.6$ and three values of $U/\pi\Gamma$ across the sign-reversal line (magenta line in Fig. 3). (a) Spectral functions computed using the NRG, and (b) closeups on the low-ω range. (c) $\mathrm{Im}\,\Sigma$ computed using the NRG and two weak-coupling approaches. Here, $\Gamma = 0.01D$, $T = 0$. b for the NRG calculations has the sign of the slopes of the dashed lines in the figures.

ω. The results, shown in Fig. 3, reveal a change of sign of the coefficient b in $\mathrm{Im}\,\Sigma$ along a curve in the U-n plane (black line in the figure). At low $U \ll \Gamma$, the sign reversal occurs close to half filling. For U of order Γ, the sign-change point rapidly moves away from half filling. At still higher U, the slope of the black curve in the U-n plane redresses and becomes increasingly vertical for $U \gg \pi\Gamma$.

These results are fully consistent with our perturbative analysis. For very small U, the third-order term is negligibly small and the sign is constant in essentially the full $0 < n < 1$ interval. In this regime, the curve separating the different signs in the U-n plane is almost vertical and close to $n = 1$. At some value of U of order $\pi\Gamma$, the perturbation theory predicts that the third-order contribution will overtake the second-order contribution for most E_d at almost the same value of u,

and b will thus change in a wide n interval. Indeed, this seems to correspond to $U \approx 2\Gamma$ where the curve in the U-n plane abruptly changes slope and becomes almost horizontal. Around the same u, however, we enter the strong-coupling regime where the perturbation theory breaks down. Note that for large $u = U/\Gamma$ the crossover (as n increases from 0) to the "strong-coupling" domain with $b > 0$ already takes place in the mixed valent regime of the impurity model; the deep Kondo limit is confined to values of n close to 1.

We also performed the skeleton expansion to second order, which is a self-consistent calculation where the dressed Green's function is used as the propagator in the second-order term of the self-energy. This corresponds to an infinite resummation of a certain class of diagrams, which for small U reduces to the bare perturbation theory in U. The results show that the coefficient b has the same sign for any value of U and n, i.e., the sign associated with the weak-coupling limit (see Fig. 4). This can also be shown analytically by invoking the Friedel sum rule [21]—for the skeleton expansion this leads to $b/a \propto \sin(n\pi)/\Gamma$, which makes b negative for all n. The absence of sign change seems to imply that the skeleton expansion is not able to describe the transition to the dynamics expected in the strong-coupling regime, presumably because its starting point is still the noninteracting limit. On the other hand, the extremely correlated Fermi-liquid theory produces the correct sign of the scattering-rate asymmetry because it is constructed as a strong-coupling approach by projecting out the double-occupancy from the outset.

Next, we compare the crossover curve with other quantities sensitive to the magnetic behavior of the impurity. The local-moment fraction $f_{\mathrm{LM}} = n - 2\langle n_\uparrow n_\downarrow \rangle$ is equal to the expectation value of the projection operator to the singly occupied impurity state (the state which carries the spin degree of freedom). It behaves as $f_{\mathrm{LM}} = n$ in the $U \gg \Gamma$ limit, while the small-U dependence is shown in Fig. 5. None of the contours
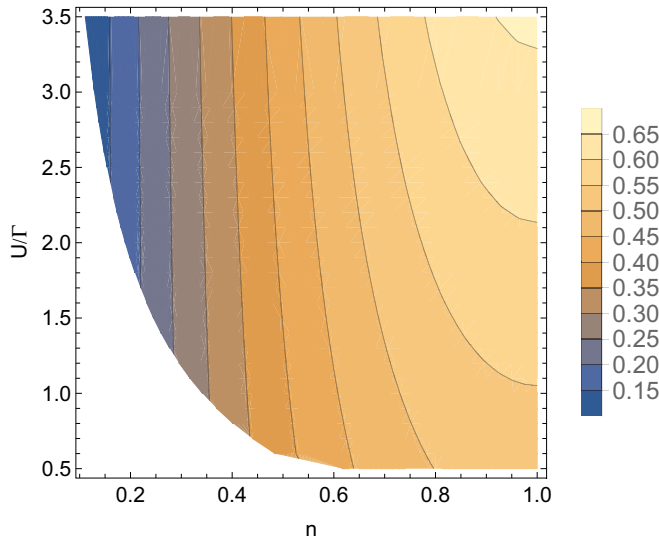
FIG. 5. Local-moment fraction $f_{\mathrm{LM}} = n - 2\langle n_\uparrow n_\downarrow \rangle$.

(isocurves) resembles the sign-reversal curve from Fig. 3. Most notably, the contours in f_{LM} approach the $n = 1$ line with zero slope and do not curve down. Other thermodynamic quantities, such as the characteristic low-energy scale of the problem defined by the temperature where the impurity entropy and the effective moment become small (i.e., the Kondo temperature in the Kondo regime), also correlate with the dependence of f_{LM} on U and n (not shown). The scattering asymmetry is thus not simply related to the degree of local-moment formation, but requires a calculation of dynamical properties.

We now discuss the relevance of these results to the low-temperature thermopower in correlated systems. Two cases need to be distinguished. In quantum dots that are directly described by the SIAM, the thermopower is determined by the asymmetry of the spectral function around the Fermi level, i.e., its Fermi-level slope [22–24]. The asymmetry of the particle-hole scattering is not important as such, as it only enters as one factor that affects the spectral-function slope. The situation is different for bulk systems described by the Hubbard model that map within the dynamical mean-field theory (DMFT) approximation to a SIAM with a self-consistently defined hybridization function [25–31]. There, the thermopower is given by the "leading" term proportional to the Fermi-level slope of the transport function that is "corrected" by a term proportional to the coefficients of the cubic terms in Im Σ. This is actually an order 1 correction [29,30], which may become dominant close to half filling. Due to the DMFT self-consistency, this term has a complex dependence on specific details of the problem [shape of the noninteracting density of states (DOS), doping level, strength of the interaction compared to the critical U_{c2} of the Mott metal-to-insulator transition]. We plan to present a study of these in a separate publication.

In conclusion, we uncovered a crossover line in the phase diagram of the single-impurity Anderson model with a flat hybridization function which corresponds to a change in the scattering dynamics. On one side of this line the impurity behaves as a weakly renormalized resonant level, and on the other side as a magnetic impurity. On the weakly correlated side, the particlelike excitations scatter more strongly than the holelike excitations, while the opposite is the case on the strongly correlated side. This crossover might be directly observable in quantum dot experiments [32,33] provided that the spectral function can be measured in a sufficient energy window so that the reconstruction of the full Green's function $G(\omega)$ is possible via the Kramers-Kronig transformation: Assuming that the hybridization function is approximately constant close to the Fermi level, the particle-hole scattering asymmetry can be easily extracted from Im$[G(\omega)^{-1}]$. The predicted almost exact particle-hole symmetry of the scattering rate along the crossover line in the U-n plane should make it an interesting feature to test for in experiments on magnetic adsorbates and quantum dots.

[1] G.-H. Gweon, B. S. Shastry, and G. D. Gu, Extremely Correlated Fermi Liquid Description of Normal State ARPES in Cuprates, Phys. Rev. Lett. **107**, 056404 (2011).

[2] B. S. Shastry, Dynamical Particle-Hole Asymmetry in Cuprate Superconductors, Phys. Rev. Lett. **109**, 067004 (2012).

[3] B. S. Shastry, Extremely Correlated Fermi Liquids, Phys. Rev. Lett. **107**, 056403 (2011).

[4] B. S. Shastry, E. Perepelitsky, and A. C. Hewson, Extremely correlated Fermi liquid study of the $U = \infty$ Anderson impurity model, Phys. Rev. B **88**, 205108 (2013).

[5] B. Horvatić and V. Zlatić, Perturbation expansion for the asymmetric Anderson Hamiltonian, Phys. Status Solidi **99**, 251 (1980).

[6] B. Horvatić and V. Zlatić, Perturbation expansion for the asymmetric Anderson Hamiltonian II. General asymmetry, Phys. Status Solidi **111**, 65 (1982).

[7] K. G. Wilson, The renormalization group: Critical phenomena and the Kondo problem, Rev. Mod. Phys. **47**, 773 (1975).

[8] H. R. Krishna-murthy, J. W. Wilkins, and K. G. Wilson, Renormalization-group approach to the Anderson model of dilute magnetic alloys. I. Static properties for the symmetric case, Phys. Rev. B **21**, 1003 (1980).

[9] H. R. Krishna-murthy, J. W. Wilkins, and K. G. Wilson, Renormalization-group approach to the Anderson model of dilute magnetic alloys. II. Static properties for the asymmetric case, Phys. Rev. B **21**, 1044 (1980).

[10] T. A. Costi and A. C. Hewson, Resistivity cross-over for the non-degenerate Anderson model, Philos. Mag. B **65**, 1165 (1992).

[11] W. Hofstetter, Generalized Numerical Renormalization Group for Dynamical Quantities, Phys. Rev. Lett. **85**, 1508 (2000).

[12] R. Bulla, T. Costi, and T. Pruschke, The numerical renormalization group method for quantum impurity systems, Rev. Mod. Phys. **80**, 395 (2008).

[13] H. O. Frota and L. N. Oliveira, Photoemission spectroscopy for the spin-degenerate Anderson model, Phys. Rev. B **33**, 7871 (1986).

[14] O. Sakai, Y. Shimizu, and T. Kasuya, Single-particle and magnetic excitation spectra of degenerate Anderson model with finite f-f Coulomb interaction, J. Phys. Soc. Jpn. **58**, 3666 (1989).

[15] T. A. Costi, A. C. Hewson, and V. Zlatić, Transport coefficients of the Anderson model via the numerical renormalization group, J. Phys.: Condens. Matter **6**, 2519 (1994).

[16] R. Bulla, A. C. Hewson, and Th. Pruschke, Numerical renormalization group calculation for the self-energy of the impurity Anderson model, J. Phys.: Condens. Matter **10**, 8365 (1998).

[17] V. L. Campo and L. N. Oliveira, Alternative discretization in the numerical renormalization group, Phys. Rev. B **72**, 104432 (2005).

[18] R. Peters, T. Pruschke, and F. B. Anders, A numerical renormalization group approach to Green's functions for quantum impurity models, Phys. Rev. B **74**, 245114 (2006).

[19] A. Weichselbaum and J. von Delft, Sum-Rule Conserving Spectral Functions from the Numerical Renormalization Group, Phys. Rev. Lett. **99**, 076402 (2007).

[20] R. Žitko and T. Pruschke, Energy resolution and discretization artifacts in the numerical renormalization group, Phys. Rev. B **79**, 085106 (2009).

[21] A. C. Hewson, *The Kondo Problem to Heavy Fermions* (Cambridge University Press, Cambridge, UK, 1993).

[22] R. Scheibner, H. Buhmann, D. Reuter, M. N. Kiselev, and L. W. Molenkamp, Thermopower of a Kondo Spin-Correlated Quantum Dot, Phys. Rev. Lett. **95**, 176602 (2005).

[23] T. A. Costi and V. Zlatić, Thermoelectric transport through strongly correlated quantum dots, Phys. Rev. B **81**, 235127 (2010).

[24] S. Andergassen, T. A. Costi, and V. Zlatić, Mechanism for large thermoelectric power in molecular quantum dots described by the negative-u Anderson model, Phys. Rev. B **84**, 241107(R) (2011).

[25] A. Georges, G. Kotliar, W. Krauth, and M. J. Rozenberg, Dynamical mean-field theory of strongly correlated fermion systems and the limit of infinite dimensions, Rev. Mod. Phys. **68**, 13 (1996).

[26] B. S. Shastry, Electrothermal transport coefficients at finite frequencies, Rep. Prog. Phys. **72**, 016501 (2009).

[27] B. S. Shastry, in *New Materials for Thermoelectric Applications: Theory and Experiments*, edited by V. Zlatić and A. Hewson (Springer, Dordrecht, 2013), pp. 25–30.

[28] K. Haule and G. Kotliar, Thermoelectrics near the Mott localization-delocalization transition, in *Properties and Applications of Thermoelectric Materials*, edited by V. Zlatić and A. C. Hewson (Springer, Dordrecht, 2009), p. 119.

[29] X. Deng, J. Mravlje, R. Žitko, M. Ferrero, G. Kotliar, and A. Georges, How Bad Metals Turn Good: Spectroscopic Signatures of Resilient Quasiparticles, Phys. Rev. Lett. **110**, 086401 (2013).

[30] W. Xu, K. Haule, and G. Kotliar, Hidden Fermi Liquid, Scattering Rate Saturation, and Nernst Effect: A Dynamical Mean-Field Theory Perspective, Phys. Rev. Lett. **111**, 036401 (2013).

[31] L.-F. Arsenault and A.-M. S. Tremblay, Transport functions for hypercubic and Bethe lattices, Phys. Rev. B **88**, 205109 (2013).

[32] D. Goldhaber-Gordon, J. Göres, M. A. Kastner, H. Shtrikman, D. Mahalu, and U. Meirav, From the Kondo Regime to the Mixed-Valence Regime in a Single-Electron Transistor, Phys. Rev. Lett. **81**, 5225 (1998).

[33] A. V. Kretinin, H. Shtrikman, D. Goldhaber-Gordon, M. Hanl, A. Weichselbaum, J. von Delft, T. Costi, and D. Mahalu, Spin-1/2 Kondo effect in an InAs nanowire quantum dot: Unitary limit, conductance scaling, and Zeeman splitting, Phys. Rev. B **84**, 245316 (2011).